Pharm Res (2012) 29:178–186
DOI 10.1007/s11095-011-0525-3

RESEARCH PAPER

Tumor Environment Changed by Combretastatin Derivative (Cderiv) Pretreatment That Leads to Effective Tumor Targeting, MRI Studies, and Antitumor Activity of Polymeric Micelle Carrier Systems

Kouichi Shiraishi • Yoshiko Harada • Kumi Kawano • Yoshie Maitani • Katsuyoshi Hori • Kazuyoshi Yanagihara • Misato Takigahira • Masayuki Yokoyama

Received: 28 April 2011 / Accepted: 29 June 2011 / Published online: 26 July 2011

ABSTRACT

Purpose To evaluate effect of a vascular disrupting agent, a combretastatin derivative (Cderiv), on tumor targeting for polymeric micelle carrier systems, containing either a diagnostic MRI contrast agent or a therapeutic anticancer drug.

Methods Cderiv was pre-administered 72 h before polymeric micelle MRI contrast agent injection. Accumulation of the MRI contrast agent in colon 26 murine tumor was evaluated with or without pretreatment of Cderiv by ICP and MRI.

Results Significantly higher accumulation of the MRI contrast agent was found in tumor tissues when Cderiv was administered at 72 h before MRI contrast agent injection. T_1-weighted images of the tumor exhibited substantial signal enhancement in tumor area at 24 h after the contrast agent injection. In T_1-weighted images, remarkable T_1-signal enhancements were observed in part of tumor, not in whole tumor. These results indicate that Cderiv pretreatment considerably enhanced the permeability of the tumor blood vessels. Antitumor activity of adriamycin encapsulated polymeric micelles with the Cderiv pretreatment suppressed tumor growth in 44As3 human gastric scirrhous carcinoma-bearing nude mice.

Conclusions Pretreatment of Cderiv enhanced tumor permeability, resulting in higher accumulation of polymeric micelle carrier systems in solid tumors.

KEY WORDS Cderiv · MRI study · polymeric micelle MRI contrast agent · tumor permeability · tumor vascular disrupting agent

ABBREVIATIONS

ADR-micelle	adriamycin-encapsulating polymeric micelle
Cderiv	(Z)-N-[2-methoxy-5-[2-(3,4,5- trimethoxy-phenyl)vinyl] phenyl]-L-serinamide hydrochloride
DLS	dynamic light scattering

Y. Harada
Kanagawa Academy of Science and Technology
Yokoyama "Nano-medical Polymer" Project
KSP East 404, Sakado 3-2-1, Takatsu-ku
Kawasaki, Kanagawa 213-0012, Japan

K. Kawano • Y. Maitani
Institute of Medicinal Chemistry Hoshi University
2-4-41 Ebara, Shinagawa-ku, Tokyo 142-8501, Japan

K. Hori
Department of Vascular Biology, Division of Cancer Control
Institute of Development Aging and Cancer, Tohoku University
4-1 Seiryomachi, Aoba-ku, Sendai 980-8575, Japan

K. Yanagihara
Department of Life Sciences, Laboratory of Molecular Cell Biology
Yasuda Woman's University Faculty of Pharmacy
6-13-1 Yasuhigashi, Asaminami-ku, Hiroshima, 731-0153, Japan

M. Takigahira
Central Animal Laboratory
National Cancer Center Research Institute
5-1-1 Tsukiji, Chuo-ku, Tokyo 104-0045, Japan

M. Takigahira
Shien Laboratory National Cancer Center Hospital
Tokyo, Japan

K. Shiraishi • M. Yokoyama (✉)
Medical Engineering Laboratory, Research Center for Medical Science
The Jikei University School of Medicine
Nishi-shinbashi 3-25-8, Minato-ku, Tokyo 105-8461, Japan
e-mail: masajun2093ryo@jikei.ac.jp

DOTA	1,4,7,10-Tetraazacyclododecane-1,4,7, 10-tetraacetic acid
EDC	1-ethyl-3-(3-dimethylaminopropyl) carbodiimide hydrochloride
EPR effect	enhanced permeability and retention effect
GPC	gel permeation chromatography
ICP	inductive coupled plasma
MRI	magnetic resonance imaging
MWCO	molecular weight cut-off
PEG-P(Lys)	poly(ethylene glycol)-b-poly(L-lysine)
ROI	region of interest
TGF-β	transforming growth factor β
TR/TE	repetition time/echo time

INTRODUCTION

Nowadays, targeting potential anticancer drugs to solid tumors by means of nanocarriers is a promising tool to maximize anticancer activity. This entire strategy for tumor targeting is based on the enhanced permeability and retention (EPR) effect (1,2). It is a well-known phenomenon that solid tumors have leaky blood vessels, namely, macromolecules of more than 40 kDa show substantial extravasation from the leaky tumor blood vessels, resulting in a large amount of accumulation in solid tumors. Many researchers have focused on macromolecular drugs that have sizes in the nanometer region to develop selective tumor targeting through the EPR effect (3). Improvement of pharmacokinetics of poorly soluble anticancer drug by means of such nano-sized drug carriers achieved long-circulation of the drug in blood which is necessary for selective tumor targeting through the EPR effect. This selective drug targeting leads to improved chemotherapy of the anticancer drug and diminishes negative side effects.

A doxorubicin encapsulated in liposome covered with poly(ethylene glycol) on the surface was approved as Doxil for treatment of Kaposi sarcoma (4). Polymer therapeutics, such as polymer-drug conjugate and polymeric micelle carriers, have been developed (5,6).

However, in our recent study on transparent chambers and a vital microscopic systems, we obtained some additional knowledge about EPR-based targeting system (7). That study examined the permeability of FITC-labeled polymeric micelles at different tumor growth stages relative to Yoshida ascites sarcoma in LY80. The FITC-labeled polymeric micelle was distributed in vessels at the interface between normal and tumor tissues, and the interface between tumor tissues and necrotic areas. It was found that the polymeric micelle accumulated in necrotic areas with dysfunction of the circulatory system. The study showed that the polymeric micelle was not accumulated in 1 mm of the microtumor without necrotic areas. This observation indicates that the tumor blood vessels in microtumors did not leak nanocarriers as compared with the advanced tumor model for common antitumor activity experiments.

Combretastatin A-4 is known as an anticancer drug that acts to tubulin by disrupting tumor vessels (8–18). One of the combretastatin A4 derivatives, Cderiv, was developed by Hatanaka *et al.* and Ohsumi *et al.* in 1998 (Fig. 1a) (10,11). Cderiv also exhibited a powerful vascular disrupting effect by intraveneous injection (8–10). The vascular disrupting effect is induced by strong interruption of tumor blood flow, which prevents nutrient supply to solid tumors and leads to necrosis in tumors (15–18). Recently, our research showed that Cderiv changed microenvironments of microtumors so that the new environments were similar to the environments characteristic of advanced tumors (19). Namely, the treatment of Cderiv induced the EPR effect in 1 mm of microtumors. A detailed whole mechanism of combretastatin A-4 derivatives including Cderiv is not completely understood yet; however, morphological and functional alternations have been seen in endothelial cells (15). Most likely, Cderiv acts indirectly in contractile arterioles of tumors, rather than directly on tumor vessels. This Cderiv pretreatment would be a new methodology to enhance EPR-effect-based delivery of therapeutic agents, as well as diagnostic agents.

Evaluation of pharmacokinetics, biodistribution, and especially drug delivery efficiency by non-invasive imaging techniques has recently become more important (20–22). Of several modalities, such as PET, CT, and MRI, MRI is a non-invasive method for three-dimensional images with high spatial resolution. Paramagnetic gadolinium chelates, such as gadolinium(III) chelates, are often used as MRI contrast agents to enhance the signal in target tissues where the contrast agents are localized (23).

A previous report on a polymeric micelle MRI contrast agent showed passive accumulation in a solid tumor, resulting in intensive enhancement of T_1-weighted signals in the tumor tissues (24). This MRI contrast agent exhibited similar pharmacokinetics as compared to a polymeric micelle anticancer drug carrier, adriamycin-encapsulating polymeric micelle (ADR-micelle) (25,26). Their structures are shown in Fig. 1b and c. As well as the pharmacokinetics, biodistribution including tumor accumulation of the MRI contrast agent was similar to that of the ADR-micelle. For example, 24.6% and 22.5% of injected dose of the ADR-micelle and the polymeric micelle MRI contrast agent were found in blood at 24 h after intravenous injection, respectively. Accumulations in C26 tumor tissues were 9.6%ID/g and 6.1%ID/g at 24 h for the ADR-micelle and the contrast agent, respectively. These results indicated that the tumor diagnosis by means of the polymeric micelle MRI contrast agent can help to predict the targeting efficiency

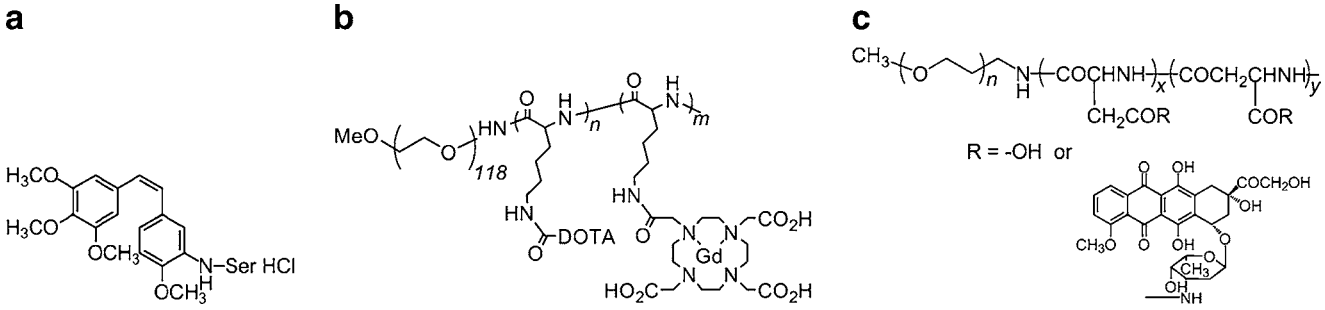

Fig. 1 Structure of (**a**) Cderiv, (**b**) polymeric micelle MRI contrast agent, and (**c**) ADR-micelle.

of the anticancer-drug-encapsulating polymeric micelle, such as the ADR-micelle.

The combination of a therapeutic drug and a diagnostic contrast agent incorporated in the same carrier system can be considered effective in the evaluation of therapeutic efficacy. This system would be a great potential for improvement of therapeutic efficacy, called as "theragnosis."

Cderiv was used to enhance permeability for improvement of the tumor targeting efficiency of a polymeric micelle carrier system. We evaluate in the present study whether Cderiv pretreatment enhances the tumor targeting of the polymeric micelle MRI contrast agent and the adriamycin-encapsulated polymeric micelle. The current study performed an MRI to evaluate the signal intensities in the tumor area. Antitumor activity was studied when this combination of the Cderiv pretreatment with ADR-micelles was used on 44As3-bearing mice (27).

MATERIALS AND METHODS

Preparation of Polymeric Micelle MRI Contrast Agents

Preparation of a polymeric micelle MRI contrast agent was reported previously (24). Briefly, a polymerization of Lys(Z) *N*-carboxy anhydride from PEG-NH_2 (Mw = 5,200) gave a poly(ethylene glycol)-b-poly[ε-(benzyloxycarbonyl)-L-lysine] (PEG-P(Lys(Z)). PEG-P(Lys(Z)) was dissolved in trifluoroacetic acid. Anisole and methanesulfonic acid were added to the solution. The mixture was stirred for 1 h to hydrolyze the protecting group. The solution was diluted with distilled water, then the excess of acid was extracted with diethylether until an organic layer became neutral. The obtained aqueous layer was neutralized by an addition of triethylamine, and dialyzed against 0.02 N NaOH and distilled water against SpectraPor 6 (MWCO = 1 k) membrane. Lyophilization gave white powder of PEG-P(Lys).

The obtained a poly(ethylene glycol)-b-poly(L-lysine) (PEG-P(Lys)) was a fully conjugated using mono *N*-hydroxysuccinimide ester of 1,4,7,10-Tetraazacyclododecane- 1,4,7,10-tetraacetic acid (DOTA) (1.3 eq *vs* lysine residues) and triethylamine in dried DMF. The reaction mixture was stirred overnight at 50°C. The resulting mixture was first dialyzed against 0.02 N HCl and then against distilled H_2O 5 times. The obtained polymer was dissolved in H_2O at a polymer concentration higher than 15 mg/mL and dialyzed against H_2O 3 times. Lyophilization gave poly(ethylene glycol)-*b*-poly(L-lysine-DOTA) (PEG-P(Lys-DOTA)) as white powder.

The conjugation was confirmed by ^{1}H-NMR under an alkali condition (pH > 10 in D_2O). The conjugated number of DOTA moiety was calculated from peak ratio between CH_2 protons of PEG at 3.73 ppm and 26H of DOTA and lysine protons in the range between 3.36 and 2.18 ppm.

The DOTA-conjugated block copolymer, PEG-P(Lys-DOTA), was mixed with $GdCl_3 \cdot 6H_2O$ at 50°C for 3 h in the range of pH 6–6.5. After several dialyses against water, Gadolinium-chelated PEG-P(Lys-DOTA-Gd) was obtained. ICP (SPS7800, SII Nano Technology Inc., Tokyo, Japan) was used for the determination of gadolinium content in the polymer. This block copolymer formed a polymeric micelle in an aqueous solution, and we detected the formation of polymeric micelle by DLS and GPC analysis.

Preparation of Adriamycin-Encapsulated Polymeric Micelles (ADR-micelles)

An adriamycin (ADR)-encapsulated polymeric micelle (ADR-micelle) was prepared according to a previously reported procedure (24,25). First, a block copolymer, poly (ethylene glycol)-*b*-poly(aspartic acid) (PEG-P(Asp)) (PEG_{Mw} = 12,000, Asp unit = 19), was synthesized from poly(ethylene glycol)-*b*-poly(β-benzyl L-aspartate). ADR was chemically conjugated to the aspartic acid of the block copolymer by EDC-mediated coupling reaction (63% conjugation to Asp unit). Then, free ADR was physically encapsulated in the block copolymer, which formed a polymeric micelle. ADR·HCl was dissolved in DMF with 1.3 equivalents of triethylemiane (*vs* ADR·HCl), and the ADR solution was mixed with the chemically ADR-

conjugated PEG-P(Asp-ADR). The mixture was stirred for 2 h at room temperature. The mixture was dialyzed with SpectraPor6 membrane against distilled water. The obtained solution was concentrated by polyethersulfone ultrafiltration membrane (MWCO = 100 k) equipped with an ultrafiltration unit (Amicon, Stirred Ultra Filter Cell). Physically encapsulated ADR was determined by an HPLC system (LC-2000 series, Jasco, Tokyo, Japan) equipped with a μBondasphere (Waters, Tokyo, Japan) column in acetonitrile/H_2O (including 1% of acetic acid) as an eluent. ADR was detected by measuring the absorbance at 485 nm. The conjugated ADR was worked only for stable encapsulation of free ADR, and no release of free ADR from the conjugate was found (28). We discussed only the physically encapsulated ADR for the determination.

MRI Study of Colon 26 CDF_1 Mice

Isoflurane (1.0–1.5%) was used for anesthesia in the MRI study. CDF_1 female mice bearing a colon 26 tumor (n=4) were intravenously injected with Cderiv (Tokyo Kasei Kogyo Co.) at a dose of 20 mg/kg. The size of the tumors was 50–150 mm^3. Either 72 h or 24 h from the Cderiv pretreatment, polymeric micelle MRI contrast agent was injected at a dose of 0.05 mmol Gd/kg into a mice tail vein.

MR images were taken with a Varian NMR system at 9.4T magnetic field. We performed a T_2-weighted fast spin echo (TR = 2,500 ms, ETL = 8, ESP = 4, effective TE = 48) and a T_1-weighted gradient echo (TR/TE = 8.0/4.2, flip angle = 30°, field of view of 50 × 30 mm, a matrix size of 192 × 192, and 2 mm for coronal thickness, and TR/TE = 8.0/4.5, flip angle = 30°, field of view of 45 × 45 mm, a matrix size of 192 × 192, and 2 mm for axial thickness). The signal intensity of the ROI was compared with the intensity of a stock solution of 0.1 mM gadolinium ion in agarose gel. For quantitative determination of gadolinium content in colon 26 tumor, the tumor samples were dissolved in the acid mixture of 98% H_2SO_4 and 62% HNO_3, and oxoammonium salt (1:2:1, v:v:v), and then were determined by means of ICP. For normalized signal intensity relative to the T_1-weighted images, the tumor area was selected as a ROI. The signal intensity of the ROI was compared with the intensity of a stock solution of 0.1 mM gadolinium ion in agarose gel. The relative signal intensity of the ROI at 24 h after the MRI contrast agent injection was compared to the signal intensity before the injection.

In Vivo Antitumor Activity

Antitumor activity against solid tumors was evaluated in human gastric scirrhous carcinoma 44As3-bearing nude mice. Tumor cells (44As3, 5.0×10^5) were transplanted into BLAB/C female nude mice (n=6) subcutaneously. BALB/c female nude mice bearing the 44As3 tumor were intravenously injected with Cderiv at a dose of 20 mg/kg at 10 days after the transplantation of 44As3 cells. ADR-micelles were injected at a dose of 10 mg/kg of physically entrapped ADR at 24 h after the Cderiv pretreatment. The mice in all cases were survived after the experiments finished at day 25. The tumor volumes and the body weights were measured at defined time intervals until 25 days after the drug treatments. The tumor volumes were calculated as follows: volume = $1/2LW^2$, where L is the long diameter and W is the short diameter of a tumor.

Animals

Five-week-old CDF_1 female mice were purchased from the Sankyo Labo Service Corporation, Tokyo, Japan. Six-week-old BALB/c female mice were purchased from CLEA Japan, Inc. All animal experiments were carried out in accordance with the guidelines of the Guiding Principles for the Care and Use of Laboratory Animals.

RESULTS AND DISCUSSION

Synthesis

Our polymeric micelle MRI contrast agent was used to observe the effect of Cderiv on tumor targeting. The Gd-DOTA-conjugated poly(ethylene glycol)-b-poly(L-lysine) block copolymer (PEG-P(Lys-DOTA-Gd)) formed a polymeric micelle as detected by means of DLS and GPC. This stably formed polymeric micelle exhibited both the characteristic long circulation in the blood and enough tumor accumulation to obtain MRI signals in the tumor tissue of colon 26-bearing mice, as reported previously (24). The blood half-lives of the polymeric micelle MRI contrast agent were 6.7 h and 18.4 h for α- and β-phases, respectively. This polymeric micelle MRI contrast agent exhibited pharmacokinetics behavior similar to that of an adriamycin-encapsulated polymeric micelle (ADR-micelle) (25,26). The advantage of this MRI contrast agent for the present work is that the MRI contrast agent informs us of the position and the amount of such a polymeric micelle MRI contrast agent in the tumor tissues, namely prediction of the drug targeting efficacy of ADR-micelle can be obtained.

Accumulation of Polymeric Micelles into Colon 26-Bearing Mice

Dose dependencies of Cderiv on tumor blood flow were evaluated previously (12). Intravenous injection of 1 and 3 mg/kg of Cderiv increased mean arterial blood pressure

for 2–3 h. The tumor blood flow was significantly decreased and was recovered in 2–4 h. However, the increased blood pressure at the dose of 10 mg/kg of Cderiv was maintained for 4–5 h, and the tumor blood flow was completely shut off among 8 h experiment. More than dose at 10 mg/kg of Cderiv caused long lasting tumor blood flow stasis for targeting of anticancer drug or diagnostic agent. Cderiv was intravenously injected at a dose of 20 mg/kg. The tumor blood flow stasis at this dose was reported to have continued for more than 6 h (13).

After the tumor blood flow stasis, some of the blood flows in the tumor vessels were recovered, and the others were not. Previous results showed that the Cderiv pretreatment remarkably enhanced permeability of the recovered and surviving tumor blood vessels (19). First, our polymeric micelle MRI contrast agent was injected at 72 h after Cderiv injection. The tumor tissues were taken out at 24 h after the contrast agent injection to determine gadolinium content in the tumor tissues by means of ICP measurement. As shown in Fig. 2a, significantly higher accumulation of the contrast agent was observed when Cderiv was pre-administered (9.8 ± 0.8%ID/g for the Cderiv treatment ($n=3$) *vs* 5.6 ± 1.0%ID/g tumor for the control ($n=5$), p value <0.001). This higher accumulation was due chiefly to the enhancement of the tumor vascular permeability induced by the Cderiv pretreatment, as observed in previous vital microscopic systems.

Then, time intervals of the Cderiv pretreatment were compared. When the polymeric micelle MRI contrast agent was injected at 24 h after the Cderiv pretreatment, 4.7 ± 1.6%ID/g tumor tissues of the accumulation of the contrast agent were observed, as shown in Fig. 2b. However, when the contrast agent was injected at 72 h after the Cderiv injection, much higher accumulation in the tumor tissues was observed as described above (8.0 ± 2.5%ID/g tumor tissues). This lower accumulation of the contrast agent at 24 h was probably because of the ongoing blood flow stasis effect of Cderiv at this dose. Actually, the damage that the disrupting effect had on the tumor tissues was significant at 24 h after the Cderiv pretreatment in the case of the LY80 tumor model, and probably the contrast agent was not delivered effectively to tumor tissues because of poor tumor blood flow (19). However, at 72 h after the Cderiv pretreatment, the recovered tumor blood flow exhibited remarkable extravasation. This may explain why the polymeric micelle MRI contrast agent exhibited much higher accumulation in the tumor tissues at 72 h after the Cderiv pretreatment.

Enhancement of fluorescence intensities in the tumor tissues indicated the extravasation of FITC-labeled polymeric micelles from the tumor blood vessels (19); however, this fluorescence measurement was typically not quantitative analysis. Previous report used FITC-labeled polymeric micelles to observe the extravasation into tumor tissues. The polymeric micelle formed from FITC-labeled poly (ethylene glycol)-b-poly(b-benzyl L-aspartate) (PEG-PBLA-FITC, molecular weight, 15,300; Mw of PEG chain, 12,000; number of BLA units, 14.0). The size of FITC-labeled polymeric micelles exhibited 48.2 ± 8.8 nm (the weight-average diameter $\pm$ SD). Enhancement of fluorescence intensities at both 24 h and 72 h after the pretreatment in the tumor tissues indicated the extravasation of FITC-labeled polymeric micelles from the tumor blood vessels (19); however, this fluorescence study was not of as quantitative measurements as measurements by means of ICP. Both cases exhibited the extravasation of FITC-labeled polymeric micelles; however, MRI as well as ICP measurement gave a quantitative amount of the polymeric micelle MRI contrast agent in the tumor tissues. Even though such fluorescence data exhibited the extravasation of polymeric micelles from the tumor blood vessels both 24 h and 72 h after the Cderiv treatment, the exact amount of the extravasated polymeric micelles in the tumor tissues was not measured. In contrast, the amount of the MRI contrast agent in tumor tissues at 72 h after the Cderiv pretreatment was quantitatively obtained through measurements of gadolinium amounts by means of ICP. A larger accumulation of 72 h post the Cderiv pretreatment was found than that of at 24 h, as shown in Fig. 2b. However, the nature of the tumor blood vessels' permeability by means of the Cderiv pretreatment remains unclear; it is thought to depend on tumor type and size. In colon 26 case, an accumulation of the polymeric micelle MRI contrast agent significantly enhanced at 72 h after the Cderiv pretreatment.

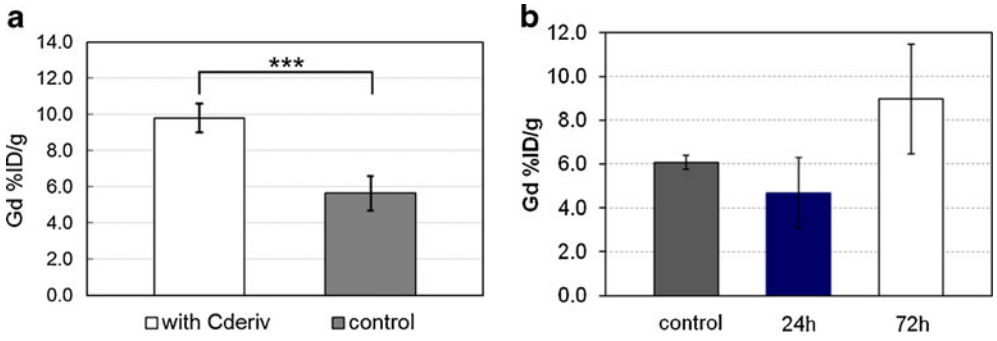

Fig. 2 Time interval effect of the Cderiv pretreatment on an accumulation of the polymeric micelle MRI contrast agent in colon 26 tumor tissues. (**a**) Either the Cderiv pretreatment at 72 h before the contrast agent injection ($n=3$) or without the treatment ($n=5$). (**b**) Control ($n=3$), the pretreatment at 24 h ($n=4$), and at 72 h ($n=4$), respectively. *** indicates P-value <0.001 (student's t-test).

MRI Study of Cderiv Pretreated Mice

Administration of Cderiv affected tumor vascular permeability, as we previously reported (19). An MRI study of the time interval study as shown in Fig. 2a was performed to observe accumulation of our polymeric micelle MRI contrast agent with the Cderiv pretreatment. When this contrast agent was used for tumor imaging in colon 26-bearing mice, a significant signal enhancement on the tumor T_1-weighted image was observed at 24 h (24). As described above section "Accumulation of Polymeric Micelles into Colon 26-Bearing Mice," in Fig. 2a, the significant difference of the accumulation of the contrast agent was found when Cderiv was pretreated at 72 h before the contrast agent injection. Figure 3 shows the axial T_1-weighted image of the tumor region (yellow circle) (a) with Cderiv treatment and (b) without treatment. A more than 2-fold (2.2 times) signal enhancement in the tumor region was observed at 24 h after the contrast agent injection (Fig. 3a). Without Cderiv treatment, 1.6 times of the signal enhancement was observed at 24 h after the injection compare to the before injection.

As well as the axial T_1-weighted image, the coronal slices exhibited characteristic images in the tumor tissues. Relatively high signal intensities were observed in the tumor-specific region, as shown in Fig. 4a (arrows). As compared to the coronal T_1-weighted images (Fig. 4a), the coronal T_2-weighted images also exhibited a curved-shape high-contrast region in the tumor tissues (Fig. 4b arrows). This relatively high contrast in the T_2-weighted image was observed before the injection of the contrast agent. Most likely, this region was caused by the Cderiv pretreatment resulting in a vasogenic edema formation. The whole mechanism of combretastatins including Cderiv on tumor vascularity is not still clear. However, evidence to date indicated the mechanism of combretastatins treatment. Combretastatins affected both morphological and functional changes in endothelial cells after the injection (9,17). Combretastatins act to the endothelial cell after the injection, which involves the damage and shape change of endothelial cells (15,16). The early effect after the combretastatin treatment on tumor vascularity was an increase in the permeability to macromolecules. This increase in the permeability leads to forming edema in tissues, and this could be increased in interstitial fluid pressure. Decreasing blood fluidity and stacking red blood cells were found in blood vessels. These events lead to vasoconstriction of the tumor vascularity.

Our previous report describes that surviving or restored tumor blood vessels exhibited a remarkable enhancement of permeability of FITC-labeled polymeric micelles after the Cderiv pretreatment (19). Figure 4c shows a merged image of the coronal T_1- or T_2-weighted tumor at the same position. The high-contrast region in the T_1-weighted image (arrow) was positioned adjacent to the T_2-weighted high-contrast region (arrow heads). These results support the assertion that the extravasation of the tumor blood vessels around such a T_2-high-contrast region was remarkably

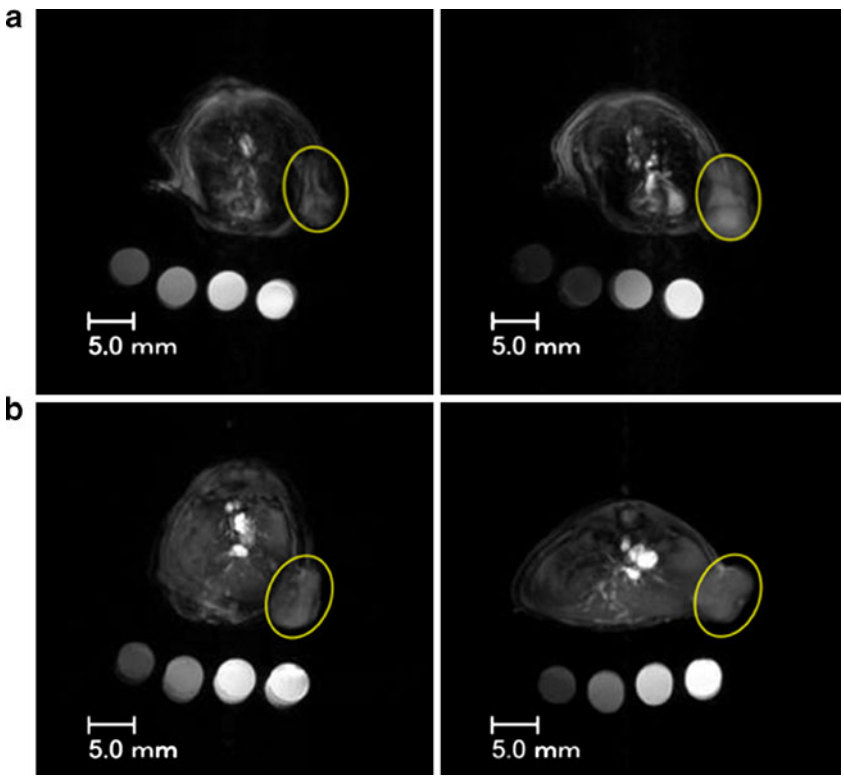

Fig. 3 Axial slices of the T_1-weighted MIP image of (**a**) Cderiv treatment at 72 h before the contrast agent injection (*left*) before and (*right*) 24 h, (**b**) without treatment (*left*) before and (*right*) 24 h.

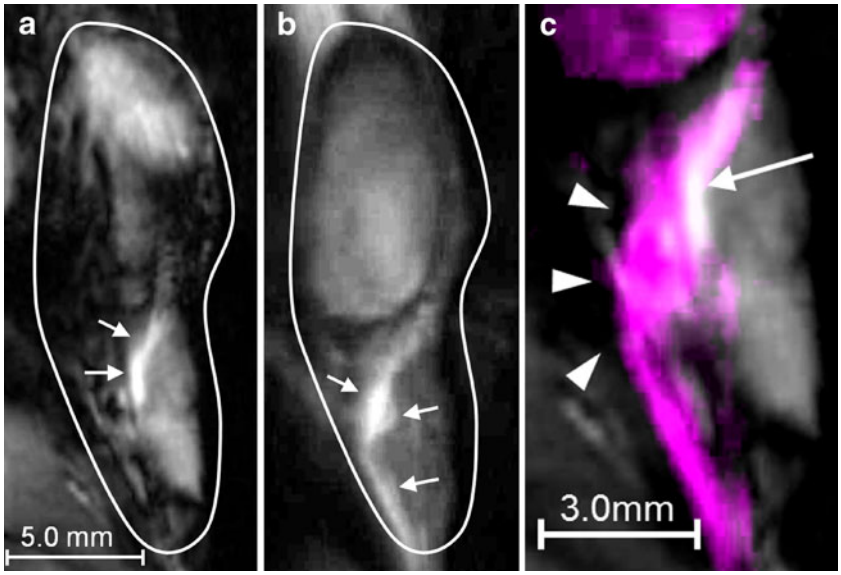

Fig. 4 Coronal slices of tumor area of (**a**) the T_1-weighted image and (**b**) the T_2-weighted image at 24 h after the injection. (**c**) A merged image of the T_1-weighted scenario (*gray*) and the T_2-weighted scenario (*magenta*) of the expanded tumor area. *Arrows* and *arrow heads* indicate the intense region of the T_1-weighted and the T_2-weighted images, respectively.

enhanced. One related result was a higher concentration of the polymeric micelle MRI contrast agent in the tumor tissues. So far, there have been no reports of an accumulation of nanoparticles specific-regions in tumor by means of the EPR effect. In terms of tumor diagnosis, high concentrations of the MRI contrast agent in such a part of the region led to the intense signal compared with the case of homogeneous distribution in a whole region of the tumor tissues. In this report, a higher accumulation of the MRI contrast agent in the tumor tissues was obtained by means of the Cderiv pretreatment. Furthermore, such a extravasated MRI contrast agent was locally concentrated in the specific region in which Cderiv might be worked. In general, the MRI contrast agent exhibits the T_1-shortening property of water protons. The concentration of the gadolinium ion significantly affected the T_1-shortening property, which would lead to the intense signal. Consequently, the observations in such specific contrast enhancement at the solid tumor help to distinguish the normal and the diseased tissues easily.

Anticancer drugs should be distributed through the whole region of the tumor tissues. Our previous report indicates that movements of macromolecules including polymeric micelles are strongly dependent on a perfusion of the tumor tissues. Namely, tumor-tissue perfusion can distribute a locally accumulated polymeric micelle encapsulating anticancer drug in the tumor tissues.

As we described in the introduction, the Cderiv pretreatment enhances the vascular permeability of the solid tumor even in microscopic tumors. In recent reports on tumor permeability for a drug targeting system, a tumor environment change by a TGF-β receptor inhibitor (TβRI) emerged for the EPR effect enhancement. TβRI induced alternation of tumor neovasculature that lead to enhanced permeability of nanoparticles (29,30). However, function of TGF-β inhibitor is diverse, and the use of such a TGF-β inhibitor for tumor permeability must carefully address the dose and side effect. On the other hand, nitroglycerin, classical medication for angina topically or orally, was examined for the EPR effect

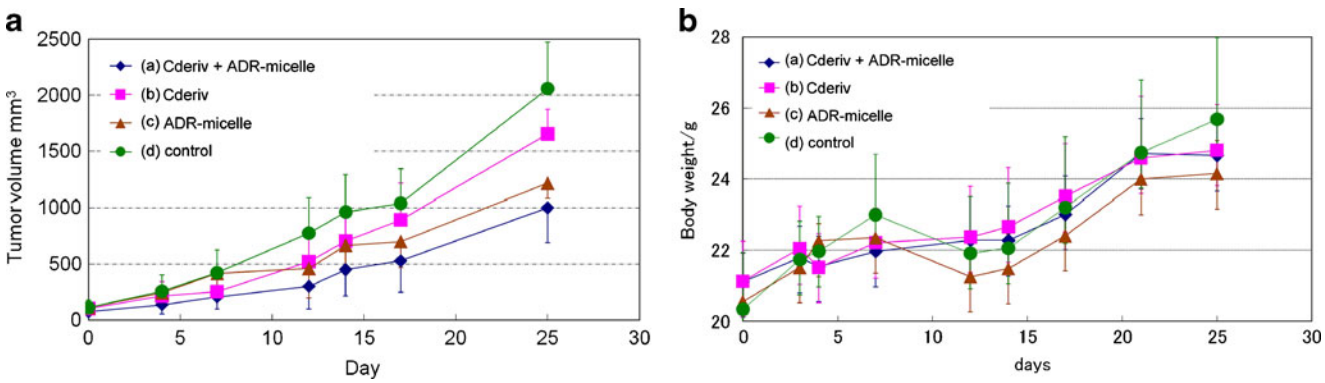

Fig. 5 (**a**) Antitumor activity of 44As3-bearing mice ($n = 6$) and (**b**) the body weight change after a single injection of (a) Cderiv + ADR-micelle, (b) Cderiv, (c) ADR-micelle, and (d) control.

enhancement. Topical application of nitroglycerin that converts to nitric oxide enhanced tumor permeability for targeting of macromolecular antitumor drugs (31,32). In contrast, Cderiv acts as a vascular disrupting agent at the tumor-specific blood capillaries. An anticancer drug targeting system supported with the Cderiv pretreatment can overcome a problem with the delivery of the nanocarriers. Because the delivery of anticancer drugs would strongly depend on the tumor vascular system, the tumor blood vessels would need to be opened to extravasate the nanocarriers. This combination greatly enhanced their permeability, resulting in the high accumulation in the solid tumor. Also, when locally accumulated, the contrast agent exhibited a relatively high signal-to-noise (S/N) ratio. This was the case of the MRI contrast agent; however, a polymeric micelle encapsulating anticancer drug could accumulate with the Cderiv pretreatment.

Antitumor Activity Relates to the Cderiv Pretreatment with ADR-Micelles Targeting 44As3 Human Gastric Scirrhous Carcinoma-Bearing Mice

Diagnosis of this scirrhous gastric carcinoma is quite difficult because of pathological features of this gastric cancer in humans. Highly progressed peritoneal dissemination or distant metastasis to lymph nodes has been observed in many cases. Due to a problem of anticancer drug targeting into this gastric cancer, this gastric scirrhous carcinoma usually generates a poor prognosis even after resection in humans. Targeting of anticancer drug into such tumor model has been highly desired (33). Antitumor activity of a single injection of ADR-micelle with the Cderiv pretreatment in 44As3 human gastric scirrhous carcinoma was evaluated by monitoring of tumor growth, as shown in Fig. 5. The dose of Cderiv and the dose of ADR-micelles were 20 mg/kg and 10 mg/kg, respectively.

Cderiv itself exhibited antitumor activity by disrupting tumor blood vessels. ADR-micelles exhibited better antitumor activity than the Cderiv treatment alone. To observe the antitumor activity, the current study used a combination of the Cderiv pretreatment with ADR-micelles. There was no statistically significant difference between the combination of Cderiv with ADR-micelles and ADR-micelles; however, this result indicates that the combination was effective for suppressing tumor growth.

In this animal experiment, we injected 10 mg/kg of ADR-micelles at 24 h after the Cderiv pretreatment. We observed enhancement of tumor permeability in LY80 tumors when Cderiv was administered at 24 h before the FITC-micelle injection (19). However, from the biodistribution study of the polymeric micelle MRI contrast agent, the contrast agent accumulated much higher concentration in the tumor tissues when Cderiv was pretreated at 72 h before the injection. In this 44As3 case, the tumor blood flow may not be recovered at 24 h after the Cderiv treatment. The effects of Cderiv on each tumor models were not known in the appropriate time to pre-treat before ADR-micelle injection.

So far, this experiment did not show serious side effects with a multiplier anticancer drug combination. In terms of the body-weight change, no difference was observed to compare with the control and the others, as shown in Fig. 5b. This combination might have an optimum time interval and dose for the antitumor activity. Also, detailed movements of the polymeric micelles after local accumulation in the tumor tissues are not yet clear; however, this combination may have a chance to be a new concept underlying nanocarrier-based antitumor drug targeting systems.

CONCLUSION

A vascular disrupting agent, Cderiv, enhanced the tumor accumulation of a polymeric micelle MRI contrast agent in the tumor tissues. An MRI shows that the signal intensities of the T_1-weighted images of the tumor area greatly enhanced at 24 h after the MRI contrast agent injection. The MRI study indicates that there was observable local accumulation of the polymeric micelles in the tumor-specific region which led to relatively high signal intensity in the tumor tissues. This T_1-relatively high region was positioned adjacent to the T_2-weighted high-contrast region. The pretreatment of Cderiv changed the tumor environment, leading to extravasation of the polymeric micelles in the tumor tissues. The combination of the Cderiv pretreatment and ADR-micelles exhibited better tumor-growth suppression of 44As3 human gastric scirrhous carcinoma. The Cderiv pretreatment enhanced tumor accumulation of the polymeric micelle MRI contrast agent. We expect a combination therapy of a polymeric micelle anti cancer drug with the Cderiv pretreatment can exhibit greater antitumor activity than a single agent's therapy through optimization in doses of both agents as well as in the interval between the two agents' injections.

REFERENCES

1. Matsumura Y, Maeda H. A new concept for macromolecular therapeutics in cancer chemotherapy: mechanism of tumoritropic accumulation of proteins and the antitumor agent Smancs. Cancer Res. 1986;46:6387–92.
2. Aliabadi HM, Lavasanifar A. Polymeric micelles for drug delivery. Expert Opin Drug Deliv. 2006;3(1):130–62.

3. Torchilin V. Tumor delivery of macromolecular drugs based on the EPR effect. Adv Drug Deliv Rev. 2011;63:131–5.
4. Amantea MA, Forrest A, Northfelt DW, Nanelok R. Population pharmacokinetics and pharmacodynamics of pegylated-liposomal doxorubicin in patients with AIDS-related Kaposi's sarcoma. Clin Pharmcol Ther. 1997;61:301–11.
5. Duncan R. Polymer conjugates as anticancer nanomedicines. Nat Rev Cancer. 2006;6:688–701.
6. Duncan R. The dawning era of polymer therapeutics. Nat Rev Drug Discov. 2003;2:347–60.
7. Hori K, Nishihara M, Yokoyama M. Vital microscopic analysis of polymeric micelle extravasation from tumor vessels: macromolecular delivery according to tumor vascular growth stage. J Pharm Sci. 2009;99(1):549–62.
8. Pettit GR, Singh SB, Hamel E, Lin CM, Alberts DS, Garcia-Kendall D. Isolation and structure of the strong cell growth and tubulin inhibitor combretastatin A-4. Experientia. 1989;45(2):209–11.
9. Tozer GM, Kanthou C, Parkins CS, Hill SA. The biology of the combretastatins as tumour vascular targeting agents. Int J Exp Pathol. 2002;83(1):21–38.
10. Hatanaka T, Fujita K, Ohsumi K, Nakagawa R, Fukuda Y, Nihei Y, *et al.* Novel B-ring modified combretastatin analogues: syntheses and antineoplastic activity. Bioorg Med Chem Lett. 1998;8(23):3371–4.
11. Ohsumi K, Nakagawa R, Fukuda Y, Hatanaka T, Morinaga Y, Nihei Y, *et al.* Novel combretastatin analogues effective against murine solid tumors: design and structureactivity relationships. J Med Chem. 1998;41(16):3022–32.
12. Hori K, Saito S, Nihei Y, Suzuki M, Sato Y. Antitumor effects due to irreversible stoppage of tumor tissue blood flow: evaluation of a novel combretastatin A-4 derivative, AC7700. Jpn J Cancer Res. 1999;90 (9):1026–38.
13. Hori K, Saito S. Microvascular mechanisms by which the combretastatin A-4 derivative AC7700 (AVE8062) induces tumour blood flow stasis. British J Cancer. 2003;89:1334–44.
14. Hori K. Cancer therapy by means of irreversible tumor blood flow stasis: Starvation tactics against solid tumors. Gene Ther Mol Biol. 2005;9:203–16.
15. Tozer GM, Kanthou C, Baguley BC. Disrupting tumour blood vessels. Nat Rev Cancer. 2005;5:423–35.
16. Griggs J, Metcalfe JC, Hesketh R. Targeting tumour vasculature: the development of combretastatin A4. Lancet Oncol. 2001;2(2):82–7.
17. Tozer GM, Prose VE, Wilson J, Cemazar M, Shan S, Dewhirst ME, *et al.* Mechanism associated with tumor vascular shut-down induced by combretastatin A-4 phosphate: intravital microscopy and measurement of vascular permeability. Cancer Res. 2001;61:6413–22.
18. Kim TJ, Ravoori M, Landen CN, Kamat AA, Han LY, Lu C, *et al.* Antitumor and antivascular effects of AVE8062 in ovarian carcinoma. Cancer Res. 2007;67(19):9337–45.
19. Hori K, Nishihara M, Shiraishi K, Yokoyama M. The combretastatin derivative (Cderiv), a vascular disrupting agent, enables polymeric nanomicelles to accumulate in microtumors. J Pharm Sci. 2010;99(6):2914–25.
20. Veiseh O, Gunn JW, Zhang M. Design and fabrication of magnetic nanoparticles for targeted drug delivery and imaging. Adv Drug Deliv Rev. 2010;62(3):284–304.
21. Sun C, Lee JSH, Zhang M. Magnetic nanoparticles in MR imaging and drug delivery. Adv Drug Deliv Rev. 2008;60(11):1252–65.
22. Liu Y, Miyoshi H, Nakamura M. Nanomedicine for drug delivery and imaging: A promising avenue for cancer therapy and diagnosis using targeted functional nanoparticles. Int J Cancer. 2007;120(2):2527–37.
23. Caravan P, Ellison JJ, McMurry TJ, Lauffer RB. Gadolinium(III) chelates as MRI contrast agents: structure, dynamics, and applications. Chem Rev. 1999;99(9):2293–352.
24. Shiraishi K, Kawano K, Minowa T, Maitani Y, Yokoyama M. Preparation and *in vivo* imaging of PEG-poly(L-lysine)-based polymeric micelle MRI contrast agents. J Contr Release. 2009;136(1):14–20.
25. Yokoyama M, Okano T, Sakurai Y, Fukushima S, Okamoto K, Kataoka K. Selective delivery of adriamycin to a solid tumor using a polymeric micelle carrier system. J Drug Targeting. 1999;7(3):171–86.
26. Yokoyama M, Miyauchi M, Yamada N, Okano T, Sakurai Y, Kataoka K. Characterization and antitumor activity of the micelle-forming polymeric anticancer drug adriamycin-conjugated poly (ethylene glycol)-poly(aspartic acid) block copolymer. Cancer Res. 1999;50:1693–700.
27. Yanagihara K, Takigahira M, Tanaka H, Komatsu T, Fukumoto H, Koizumi F, *et al.* Development and biological analysis of peritoneal metastasis mouse models for human scirrhous stomach cancer. Cancer Sci. 2004;96(6):323–32.
28. Yokoyama M, Fukushima S, Uehara R, Okamoto K, Kataoka K, Sakurai Y, *et al.* Characterization of physical entrapment and chemical conjugation of adriamycin in polymeric micelles and their design for *in vivo* delivery to a solid tumor. J Contr Release. 1998;50(1–3):79–92.
29. Kano RM, Bae Y, Iwata C, Morishita Y, Yashiro M, Oka M, *et al.* Improvement of cancer-targeting therapy, using nanocarriers for intractable solid tumors by inhibition of TGF-β signaling. Proc Natl Acad Sci USA. 2007;104(9):3460–5.
30. Minowa T, Kawano K, Kuribayashi H, Shiraishi K, Sugino T, Hattori Y, *et al.* Increase in tumour permeability following TGF-β type I receptorinhibitor treatment observed by dynamic contrast-enhanced MRI. Br J Canc. 2009;101:1884–90.
31. Seki T, Fang J, Maeda H. Enhanced delivery of macromolecular antitumor drugs to tumors by nitroglycerin application. Cancer Sci. 2009;100(12):2426–30.
32. Maeda H. Tumor-selective delivery of macromolecular drugs via the EPR effect: background and future prospects. Bioconjugate Chem. 2010;21(5):797–802.
33. Nakajima TE, Yanagihara K, Takigahira M, Yasunaga M, Kato K, Hamaguchi M, *et al.* Antitumor Effect of SN-38–releasing polymeric micelles, NK012, on spontaneous peritoneal metastases from orthotopic gastric cancer in mice compared with irinotecan. Cancer Res. 2008;68(22):9318–22.